Overexpression of Linc 4930556M19Rik Suppresses High Glucose-Triggered Podocyte Apoptosis, Fibrosis and Inflammation via the miR-27a-3p/Metalloproteinase 3 (*TIMP3*) Axis in Diabetic Nephropathy

Authors' Contribution:
Study Design A
Data Collection B
Statistical Analysis C
Data Interpretation D
Manuscript Preparation E
Literature Search F
Funds Collection G

ABCE 1 **Hong Fan**
BC 2 **Weiwei Zhang**

1 Department of Endocrinology and Metabolism, Heping Hospital Affiliated to Changzhi Medical College, Changzhi, Shanxi, P.R. China
2 Department of Endocrinology, The Second Affiliated Hospital of Dalian Medical University, Dalian, Liaoning, P.R. China

Corresponding Author: Weiwei Zhang, e-mail: zwuzty@163.com
Source of support: Departmental sources

Background: Long non-coding RNAs (lncRNAs) play vital roles in development of diabetic nephropathy (DN). The goal of our study was to investigate the functional roles of long intergenic noncoding RNA (lincRNA) 4930556M19Rik in DN.

Material/Methods: A DN cell model was constructed by exposing podocytes to high glucose (HG). A subcellular fraction assay was used to determine the level of 4930556M19Rik in the nucleus and cytoplasm of podocytes. Quantitative real-time polymerase chain reaction was used to evaluate expression of 4930556M19Rik and miR-27a-3p. Western blot assay was used to assessed levels of fibrosis-related proteins, podocin, and tissue inhibitor of metalloproteinase 3 (*TIMP3*). Flow cytometry analysis was performed to analyze cell apoptosis. Enzyme linked immunosorbent assay was used to examine secretion of inflammatory cytokines. Dual-luciferase reporter, RIP, and RNA pull-down assays were used to verify the relationship between miR-27a-3p and 4930556M19Rik or *TIMP3*.

Results: 4930556M19Rik was significantly decreased in HG-stimulated podocytes and mainly enriched in the cytoplasm of podocytes. Elevation of 4930556M19Rik hampered HG-induced cell apoptosis, fibrosis, and inflammatory in podocytes. 4930556M19Rik sponged miR-27a-3p to negatively modulate miR-27a-3p expression. MiR-27a-3p overexpression reversed the impact of 4930556M19Rik mediated cell progression in HG-induced podocytes. Moreover, *TIMP3* was the target for miR-27a-3p and miR-27a-3p inhibition slowed podocyte injury by targeting *TIMP3*.

Conclusions: 4930556M19Rik overexpression slowed HG-induced podocyte injury by downregulating miR-27a-3p and upregulating *TIMP3*.

MeSH Keywords: Apoptosis Inducing Factor • Diabetic Nephropathies • RNA, Long Noncoding

Full-text PDF: https://www.medscimonit.com/abstract/index/idArt/925361

📄 2932   🗐 —   📊 6   📚 29

Background

Diabetic nephropathy (DN) is a diabetic microvascular complication that is a major cause of chronic kidney disease [1]. The pathological features of DN include glomerular and tubular hypertrophy, glomerular basement membrane thickening, extracellular matrix (ECM) accumulation, renal fibrosis, podocyte dysfunction, and other changes in renal function and structure [2,3]. Although much progression has been made in DN, it remains critical to investigate the mechanisms by which it occurs and to develop new types of therapy for DN.

Long non-coding RNAs (lncRNAs) are a series of non-coding RNAs with >200 nucleotides (nts), which play crucial roles in diverse cellular processes [4]. Key regulatory functions of lncRNAs in human diseases, including DN, have been elucidated. For example, NEAT1 knockdown facilitates mouse mesangial cell (MC) apoptosis and hampers growth, inflammation, and fibrosis in DN [5]. MALAT1 silencing impedes high glucose (HG)-activated endothelial to mesenchymal transition (EMT) and fibrosis in human kidney-2 (HK-2) cells [6]. Li et al. showed that long intergenic noncoding RNA (lincRNA) 1700020I14Rik was reduced in mice with DN and HG-triggered MCs and 1700020I14Rik elevation suppressed MC growth and fibrosis in HG [7]. The same authors also suggested that linc 4930556M19Rik was downregulated in DN mice [7]. However, the effect and mechanism of 4930556M19Rik in DN are still unclear.

MicroRNAs (miRNAs) are another class of ncRNAs with ~22 nts that inhibit gene expression post-transcriptionally by recognizing the 3' untranslated region (3' UTR) of mRNA [8]. miRNAs have been shown to serve as essential regulators ofn DN development. For example, miR-30c-5p has an inhibitory effect on HG-stimulated renal fibrosis and EMT in DN by directly targeting janus kinase 1 (JAK1) [9]. MiR-15b-5p relieves HG-stimulated podocyte apoptosis, oxidative injury, and inflammation by interacting with Semaphorin 3A (Sema3A) [10]. MiR-503 plays a promotional role in HG-triggered podocyte injury in DN by negatively regulating E2F transcription factor 3 (E2F3) expression [11]. These findings indicate that miRNAs play dual roles in DN. Moreover, several reports have shown that miR-27a-3p contributes to damage to podocytes in DN [12,13]. Nonetheless, the precise roles and underlying mechanisms of miR-27a-3p in DN still need further exploration.

The balance of tissue inhibitor of matrix metalloproteinase (TIMP) and matrix metalloproteinases (MMPs) influences the integrity of ECM [14]. A member of the TIMP family, *TIMP3* is enhanced in kidney disease and associated with fibrosis, inflammation, and cell growth [15]. Furthermore, deficiency in *TIMP3* has been shown to aggravate progression of DN by acting as a target for miRNA [14,16]. However, the relationship between miR-27a-3p and *TIMP3* in DN remains unclear.

In this paper, we explored the effect and mechanism of 4930556M19Rik in pathogenesis of DN by using a DN cell model of HG-triggered podocytes.

Material and Methods

Cell culture and treatment

Mouse podocytes were bought from the Cell Resource Center of Peking Union Medical College (Beijing, China) and cultured in RPMI1640 medium (Gibco, Grand Island, New York, United States), treated with 1% penicillin-streptomycin (Gibco), 10% FBS (Gibco), 5 mM glucose (Sigma-Aldrich, St. Louis, Missouri, United States), and 10 U/mL recombinant mouse IFN-γ (Sigma-Aldrich) at 33°C in a humidified condition of 5% CO_2.

Podocytes were exposed to high glucose (HG; 30 mM; Sigma-Aldrich) for indicated time points or exposed to different doses of glucose (Sigma-Aldrich) for 36 h, and then subjected to subsequent experiments.

Cell transfection

The overexpression plasmid of 4930556M19Rik (4930556M19Rik) and matched control (pcDNA), siRNA targeting 4930556M19Rik (si-4930556M19Rik) and si-NC, miR-27a-3p mimics (miR-27a-3p) and miR-NC, miR-27a-3p inhibitors (in-miR-27a-3p) and in-miR-NC, siRNA targeting *TIMP3* (si-*TIMP3*) and si-NC were synthesized by GeneCopoeia (Guangzhou, China). Indicated synthetic oligonucleotides or plasmids were transiently transfected into podocytes with Lipofectamine 2000 (Invitrogen, Carlsbad, California, United States). After transfection, the DN cell model was stimulated by exposing podocytes to HG (Sigma-Aldrich) for 36 h.

Quantitative real-time polymerase chain reaction

RNA extraction was done by using TRIzol (Invitrogen). A M-MLV Reverse Transcriptase Kit (Promega, Madison, Wisconsin, United States) or miRNA 1st Strand cDNA Synthesis Kit (Vazyme, Nanjing, China) was used to reverse RNA into cNDA. Then AceQ Universal SYBR qPCR Master Mix (Vazyme) was used to perform quantitative real-time polymerase chain reaction (qRT-PCR) on an ABI 7500 PCR system. Relative expression was normalized to 18S or U6 and computed by the $2^{-\Delta\Delta Ct}$ strategy. Primer sequences were:
4930556M19Rik (Mouse):
(F: 5'-AGGGGAATTGTTGGACACAG-3' and
R: 5'-AGGAGCCTGAGCCTAGATCC-3');
miR-27a-3p (Mouse):
(F: 5'-ACACTCCAGCTGGGTTCACAGTGGCTAAG-3' and

R: 5'-CTCAACTGGTGTCGTGGAGTCCGGCAATTCAGTTGAGGCG
GAACT-3');
TIMP3 (Mouse):
(F: 5'- ACCCTTGGCCACTTAGTCCT-3' and
R: 5'-ACTGCCGCTCTTTTCTTCAA-3');
U6 (Mouse):
(F: 5'-GCTTCGGCAGCACATATACTAAAAT-3' and
R: 5'-CGCTTCACGAATTTGCGTGTCAT-3');
18S (Mouse):
(F: 5'-AGGGGAGAGCGGGTAAGAGA-3' and
R: 5'-GGACAGGACTAGGCGGAACA -3').

Subcellular fraction assay

A PARIS Kit (Invitrogen) was applied for separation of cytoplas-
mic and nuclear fractions in podocytes based on the manufac-
turer's protocols. RNAs extracted from the fractions were sub-
jected to qRT-PCR to determine levels of 4930556M19Rik, U6
and 18S. U6 and 18S served as the control nuclear transcript
and cytoplasmic transcript, respectively.

Flow cytometry analysis

After relevant transfection and treatment, podocyte apoptosis
was estimated using an Annexin V-FITC/PI Apoptosis Detection
Kit (Vazyme). Briefly, collected podocytes were washed with
cold phosphate buffered saline (Vazyme) and resuspended.
After that, cells were dyed with Annexin V-FITC and propidi-
um iodide according to the manufacturers' protocols. Podocyte
apoptosis rate was estimated with FACScan® flow cytometry.

Western blot assay

Total protein was isolated from podocytes with RIPA (Beyotime,
Shanghai, China) and quantified using a BCA Protein
Quantification Kit (Tiangen, Beijing, China). Then 30-μg pro-
teins were electrophoresed through 10% SDS-PAGE (Solarbio,
Beijing, China) and blotted on polyvinylidene fluoride. After
being blocked in 5% slim milk for 1 h, the membranes were
blotted with primary antibodies against alpha-smooth muscle
actin (α-SMA; ab32575; Abcam, Cambridge, Massachusetts,
United States), fibronectin (FN; ab2413; Abcam), collagen I
(Col I; ab34710; Abcam), podocin (ab93650; Abcam), *TIMP3*
(ab39814; Abcam) and β-actin (ab8228; Abcam) overnight at
4°C followed by interaction with horseradish peroxidase-con-
jugated secondary antibody (ab205719; Abcam) for 1.5 h at
indoor temperature. The proteins were developed with an ECL
reagent (Vazyme).

Enzyme linked immunosorbent assay (ELISA)

Following indicated transfection and treatment, the super-
natants of podocytes were collected. Then enzyme linked
immunosorbent assay (ELISA) kits (Abcam) were used to deter-
mine levels of interleukin (IL)-1β, tumor necrosis factor (TNF)-α
and IL-6, following the manufacturers' instructions.

Dual-luciferase reporter assay

Sequences of wild-type 4930556M19Rik or 3' UTR of *TIMP3*
including the binding sequences of miR-27a-3p were intro-
duced into psiCHECK-2 plasmid (Promega). Similarly, sequenc-
es of mutant 4930556M19Rik or 3' UTR of *TIMP3* lacking miR-
27a-3p binding sites were also introduced into psiCHECK-2
plasmid (Promega). The podocytes were co-transfected with
the indicated luciferase reporter plasmid (4930556M19Rik
WT, 4930556M19Rik MUT, TIMP 3' UTR WT or TIMP 3' UTR
MUT) and miR-27a-3p or miR-NC. Following transfection for
48 h, luciferase activity was assessed via the Dual-Luciferase
Reporter Assay system (Promega).

## RNA immunoprecipitation (RIP) assay

An Imprint® RNA Immunoprecipitation Kit (Sigma-Aldrich) was
used to perform an RNA immunoprecipitation (RIP) assay. In
brief, miR-27a-3p or miR-NC was transfected into podocytes.
Then the podocytes were harvested and lysed with RIP buf-
fer. Next, cell supernatants were cultivated overnight at 4°C
with magnetic beads and antibody immunoglobulin G (IgG;
Abcam) or Argonaute-2 (Ago2; Abcam). The co-precipitated
RNAs were purified followed by qRT-PCR assay for detection
of 4930556M19Rik level.

RNA pull-down assay

Wild-type or mutant 4930556M19Rik biotin-labeled probe
(Bio-4930556M19Rik WT or Bio-4930556M19Rik MUT) or Bio-
NC was transfected into the podocytes and then harvested.
Cell lysates were cultivated with streptavidin-coupled mag-
netic beads (Invitrogen) to generate probe-coated beads and
incubated overnight. The RNA complexes pulled down by the
beads were isolated and then miR-27a-3p level was deter-
mined by qRT-PCR.

Statistical analysis

All experiments were executed in triplicate. Data analysis
was done using GraphPad Prism 7. The data were exhibited
as mean±SD. Student's *t*-test or one-way analysis of variance
was used for difference analysis. I $P<0.05$ was considered sta-
tistically signifcant.
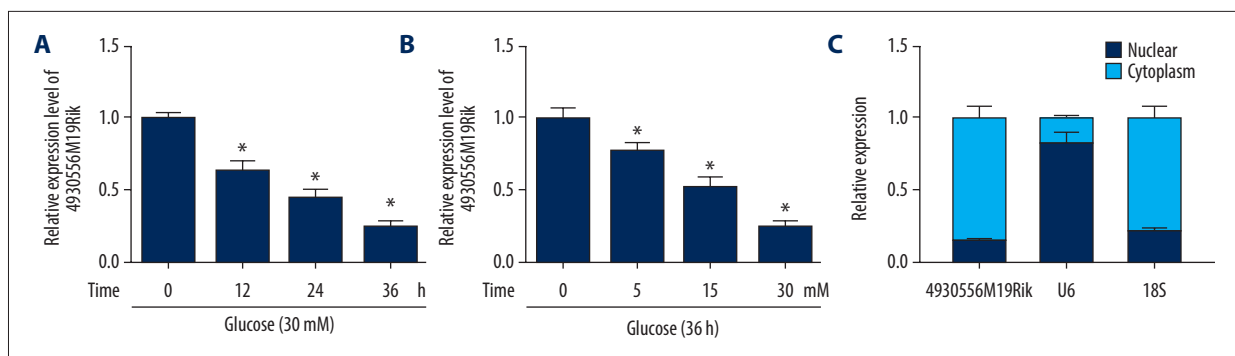
Figure 1. 4930556M19Rik level was reduced in HG-stimulated podocytes. (**A**) Expression of 4930556M19Rik in podocytes stimulated with 30-mM glucose for 0 h, 12 h, 24 h, and 36 h was determined using qRT-PCR assay. (**B**) 4930556M19Rik level in podocytes induced with 0 mM, 5 mM, 15 mM and 30 mM for 36 h was detected via qRT-PCR assay. (**C**) Following subcellular fraction, the 4930556M19Rik level in the cytoplasmic and nuclear fractions of podocytes was examined using qRT-PCR. * P<0.05.

Results

Expression of LincRNA 4930556M19Rik was low in HG-induced podocytes

First, we evaluated the effect of time on expression of 4930556M19Rik in HG (30 mM glucose)-stimulated podocytes. Decrease in 4930556M19Rik in 30-mM glucose-cultured podocytes was clearly time-dependent (Figure 1A). Moreover, 4930556M19Rik level in podocytes cultured in different concentrations of glucose (0 mM, 5 mM, 15 mM and 30 mM) was measured and the results showed a dose-dependent decrease of 4930556M19Rik level in podocytes (Figure 1B). In addition, a subcellular fractionation location assay showed that 4930556M19Rik was mainly enriched in the cytoplasm of podocytes (Figure 1C). These results suggest that 4930556M19Rik may play a role in DN.

Overexpression of 4930556M19Rik alleviated HG-induced apoptosis, fibrosis, and inflammatory response in podocytes

To explore whether 4930556M19Rik was involved in regulating the biological process of DN, podocytes were treated with 30-mM glucose (HG), 5-mM glucose+24.5-mM mannitol (NC), HG+pcDNA or HG+4930556M19Rik. As demonstrated by qRT-PCR assay, downregulation of 4930556M19Rik induced by HG was effectively reversed by transfection of 4930556M19Rik in podocytes (Figure 2A). Flow cytometry analysis indicated that HG exposure markedly triggered apoptosis of podocytes, while 4930556M19Rik overexpression reversed the impact (Figure 2B). Next, we assessed the impact of 4930556M19Rik on fibrosis in HG-activated podocytes by detecting levels of fibrosis-related proteins with Western blot assay. The results showed that HG treatment clearly elevated α-SMA, FN, and Col I levels in podocytes compared to NC groups, whereas the

impacts were all abrogated by elevation of 4930556M19Rik (Figure 2C). Moreover, the level of a podocyte-specific marker (podocin) was examined. Data from the Western blot assay showed that podocin was significantly reduced in podocytes after HG exposure, while 4930556M19Rik overexpression restored the influence (Figure 2C). Furthermore, ELISA assay indicated that secretion of inflammatory cytokines (IL-1β, TNF-α and IL-6) was strongly increased in podocytes following treatment of HG compared to NC groups, but the increase was effectively abolished by 4930556M19Rik upregulation (Figure 2D–2F). To sum up, the promotional effects on podocyte apoptosis, fibrosis, and inflammation mediated by HG treatment were abolished by 4930556M19Rik overexpression.

4930556M19Rik negatively regulated miR-27a-3p expression by direct targeting

A search of the online software diana_tools-lncbasev2 showed that miR-27a-3p shared binding sites with 4930556M19Rik (Figure 3A). Dual-luciferase reporter, RIP, and RNA pull-down assays next were performed to further determine the targeting relationship between miR-27a-3p and 4930556M19Rik. As demonstrated by dual-luciferase reporter assay, miR-27a-3p transfection markedly inhibited the luciferase activity of 4930556M19Rik WT in podocytes, and in-miR-27a-3p, transfection showed the opposite results, whereas no change was observed in 4930556M19Rik MUT groups (Figures 3B, 3C). RIP assay indicated that overexpression of miR-27a-3p drastically enriched 4930556M19Rik in Ago2 immunoprecipitation complexes in comparison with IgG groups (Figure 3D). Moreover, RNA pull-down assay showed that miR-27a-3p was markedly elevated in Bio-4930556M19Rik WT pulled down pellet in podocytes compared to Bio-NC or Bio-4930556M19Rik MUT pulled down pellet (Figure 3E). Thereafter, the miR-27a-3p level in HG-stimulated podocytes was examined with qRT-PCR, revealing that the miR-27a-3p level was higher in HG-stimulated
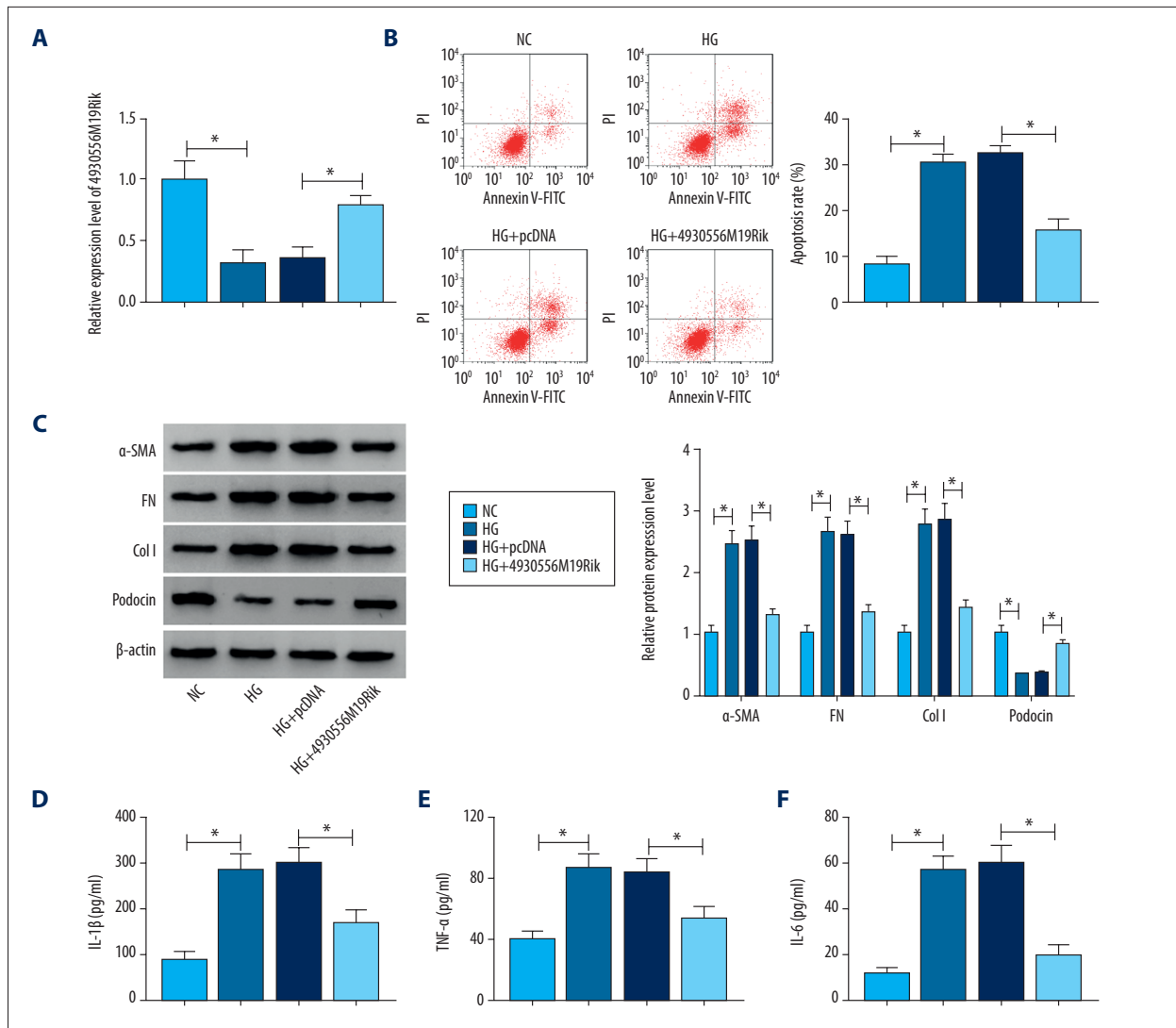
Figure 2. HG-trigged podocyte apoptosis, fibrosis and inflammation were relieved by the elevation of 4930556M19Rik. Podocytes were treated with HG (30 mM glucose), NC (5-mM glucose+24.5-mM mannitol) or transfected with pcDNA or 4930556M19Rik in HG. (**A**) 4930556M19Rik expression in podocytes was determined by qRT-PCR assay. (**B**) Apoptosis of podocytes was tested by flow cytometry analysis. (**C**) Protein levels of α-SMA, FN, Col I, and podocin were measured with Western blot assay. (**D–F**) Levels of IL-1β, TNF-α, and IL-6 were examined using ELISA kits. * P<0.05.

podocytes than in control cells (Figure 3F). In addition, we observed that 4930556M19Rik transfection led to a remarkable downregulation in miR-27a-3p expression in HG-induced podocytes, while si-4930556M19Rik transfection exhibited the opposite result (Figure 3G). Collectively, 4930556M19Rik negatively regulated expression of miR-27a-3p by direct targeting.

MiR-27a-3p overexpression restored the impacts of 4930556M19Rik on cell apoptosis, fibrosis, and inflammatory response in HG-triggered podocytes

The above results elucidated the role of 4930556M19Rik inaltering biological behaviors of podocytes by regulating

miR-27a-3p. Podocytes were treated with pcDNA, 4930556M19Rik, 4930556M19Rik+miR-NC or 4930556M19Rik+miR-27a-3p and then exposed to HG for 36 h. Transfection efficiency was evaluated by qRT-PCR. The results showed that downregulation of miR-27a-3p caused by 4930556M19Rik overexpression was effectively reversed after elevation of miR-27a-3p in HG-stimulated podocytes (Figure 4A). Podocyte apoptosis was tested with flow cytometry analysis, and suggested that the inhibitory effect of 4930556M19Rik overexpression on HG-cultured podocyte apoptosis was ameliorated by elevating miR-27a-3p expression (Figure 4B). Moreover, miR-27a-3p elevation restored the impacts on α-SMA, FN, Col I and podocin protein levels in HG-induced podocytes mediated by 4930556M19Rik (Figure 4C).
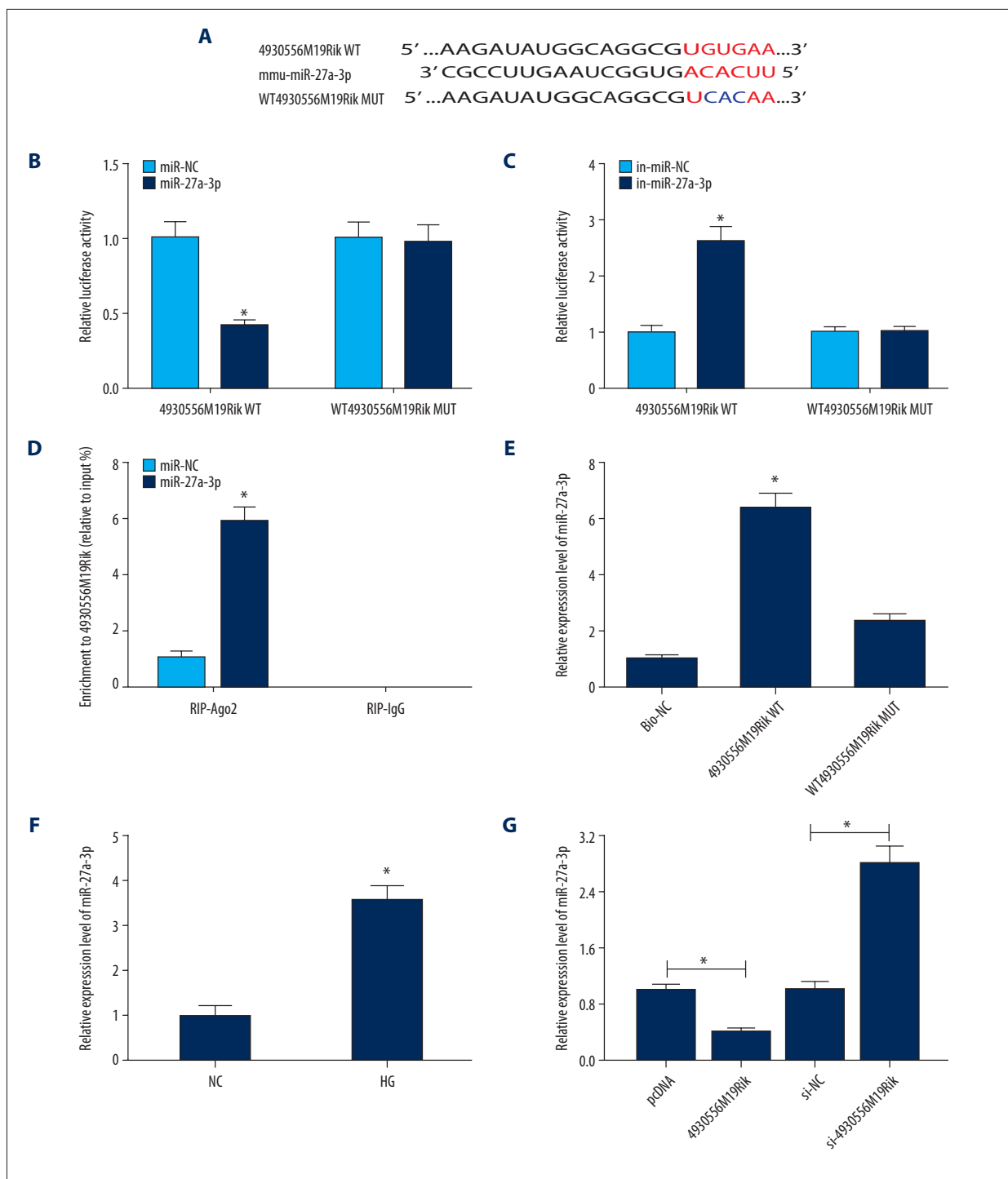
Figure 3. MiR-27a-3p was a direct target of 4930556M19Rik. (**A**) Complementary sequences between 4930556M19Rik and miR-27a-3p were predicted by diana_tools-lncbasev2. (**B, C**) Luciferase activity in podocytes co-transfected with miR-27a-3p, miR-NC, in-miR-27a-3p or in-miR-NC and 4930556M19Rik WT or 4930556M19Rik MUT was measured by dual-luciferase reporter assay. (**D**) After podocytes were transfected with miR-27a-3p or miR-NC, enrichment of 4930556M19Rik in Ago2 or IgG immunoprecipitation complexes was analyzed by RIP assay and qRT-PCR assay. (**E**) Relative expression of miR-27a-3p in podocyte lysates was determined by qRT-PCR assay following RNA pull-down assay. (**F**) MiR-27a-3p level in HG-induced podocytes and corresponding controls was detected using qRT-PCR assay. (**G**) Podocytes were transfected with pcDNA, 4930556M19Rik, si-NC or si-4930556M19Rik and then treated with HG. Next, the expression level of miR-27a-3p in podocytes was measured using qRT-PCR assay. * $P<0.05$.
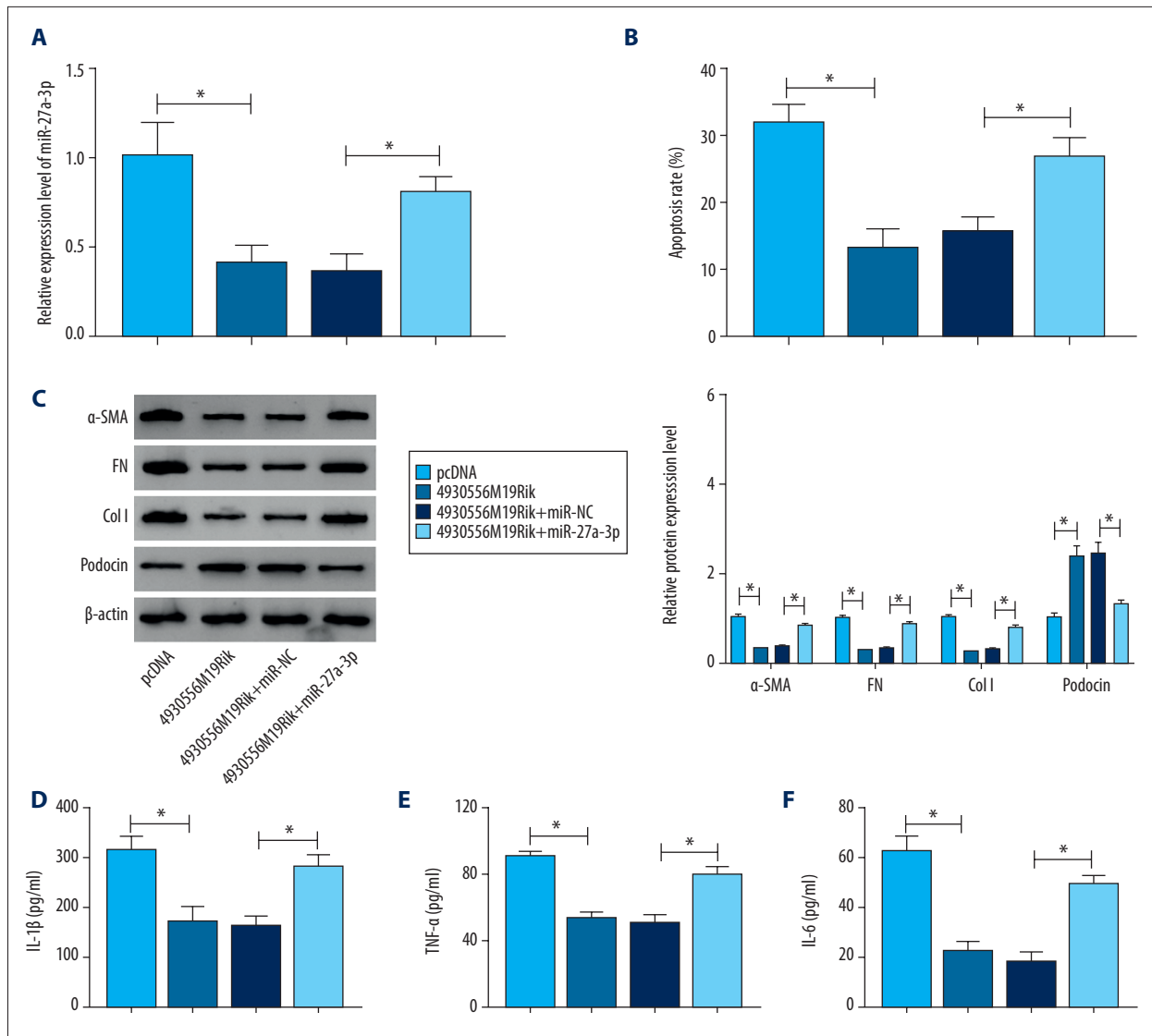
Figure 4. 4930556M19Rik overexpression suppressed cell apoptosis, fibrosis, and inflammatory response by binding to miR-27a-3p in HG-stimulated podocytes. Podocytes were transfected with pcDNA, 4930556M19Rik, 4930556M19Rik+miR-NC or 4930556M19Rik+miR-27a-3p followed by treatment of HG. (**A**) MiR-27a-3p expression in HG-induced podocytes was measured by qRT-PCR assay. (**B**) Apoptosis in HG-induced podocytes was tested by via flow cytometry analysis. (**C**) Protein levels of α-SMA, FN, Col I, and podocin in HG-induced podocytes were measured using Western blot assay. (**D–F**) Secretion of IL-1β, TNF-α, and IL-6 was examined with ELISA kits. * P<0.05.

ELISA assay showed that 4930556M19Rik overexpression led to an apparent reduction in inflammatory cytokines in HG-stimulated podocytes, whereas miR-27a-3p upregulation partially reversed the influences (Figure 4D–4F). Taken together, 4930556M19Rik overexpression attenuated HG-activated podocyte injury by interacting with miR-27a-3p.

TIMP3 was the direct target gene of miR-27a-3p

Subsequently, we further explored the underlying mechanisms of action of 4930556M19Rik and miR-27a-3p in DN. Using the

online software DianaTools-microT_CDS, *TIMP3* was observed to contain potential binding sites for miR-27a-3p (Figure 5A). Dual-luciferase reporter assay showed that miR-27a-3p and *TIMP3* 3'UTR WT co-transfection led to an obvious inhibition in the luciferase activity in podocytes, while co-transfection of in-miR-27a-3p and *TIMP3* 3'UTR WT led to marked promotion in the luciferase activity in podocytes (Figure 5B, 5C). As expected, the protein level of *TIMP3* was downregulated in HG-induced podocytes relative to control groups (Figure 5D). miR-27a-3p transfection also markedly repressed the protein level of *TIMP3* in HG-cultured podocytes compared to miR-NC groups
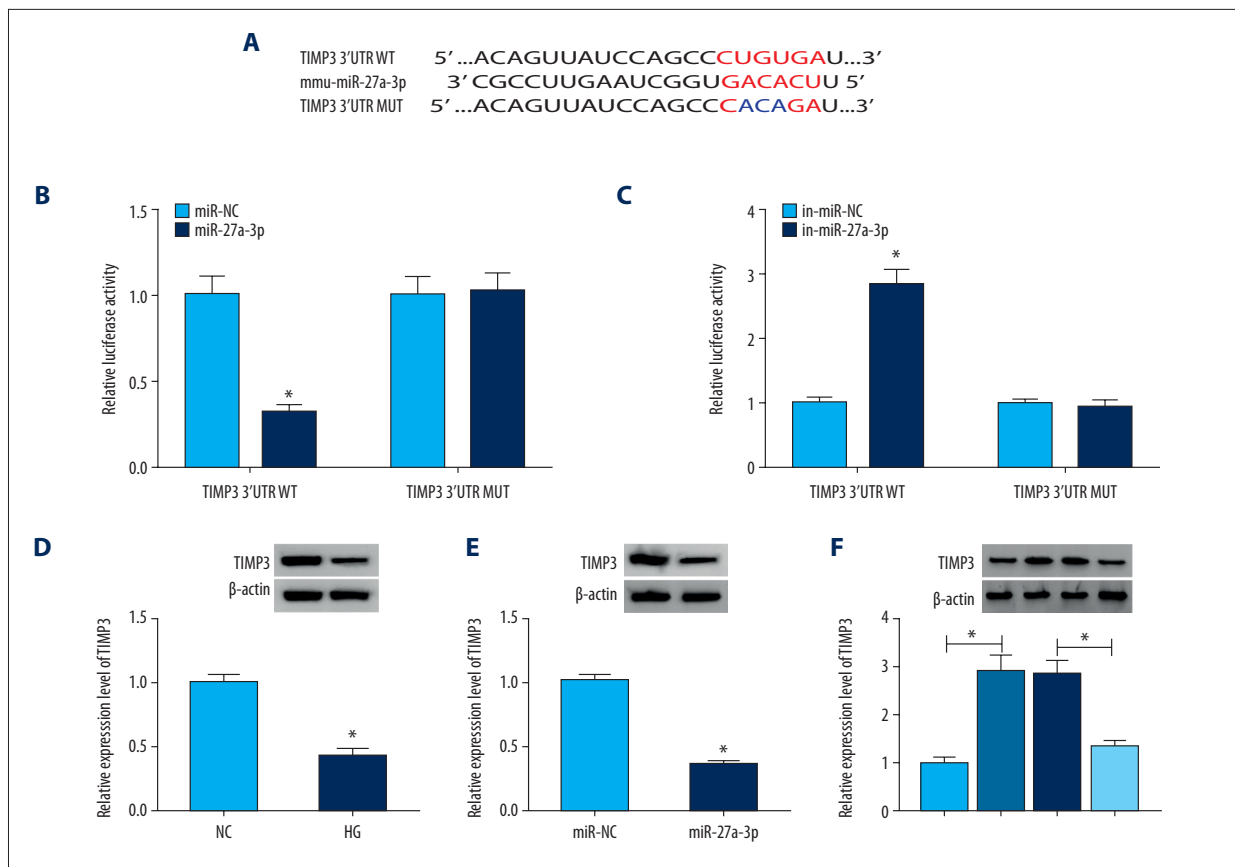
Figure 5. *TIMP3* was identified as a target gene of miR-27a-3p. (**A**) Potential binding sites between miR-27a-3p and *TIMP3* were predicted by DianaTools-microT_CDS. (**B, C**) *TIMP3* 3'UTR WT or *TIMP3* 3' UTR MUT together with miR-27a-3p, miR-NC, in-miR-27a-3p or in-miR-NC were transfected into podocytes and then the luciferase activity in podocytes was measured by dual-luciferase reporter assay. (**D**) The protein level of *TIMP3* in HG-cultured podocytes and NC groups was measured via western blot assay. (**E**) After podocytes were transfected with miR-NC or miR-27a-3p and treated with HG, the level of *TIMP3* protein was detected through Western blot assay. (**F**) Podocytes were transfected with pcDNA, 4930556M19Rik, 4930556M19Rik+miR-27a-3p or 4930556M19Rik+miR-NC and exposed to HG, then the protein level of *TIMP3* was examined by western blot assay. * P<0.05.

(Figure 5E). More importantly, we observed that 4930556M19Rik overexpression remarkably increased *TIMP3* protein level in HG-triggered podocytes, while the impact was restored by up-regulating miR-27a-3p (Figure 5F). All these outcomes demonstrated that 4930556M19Rik could positively modulate *TIMP3* expression by targeting miR-27a-3p.

Deficiency of *TIMP3* abrogated the suppressive impacts of miR-27a-3p inhibition in cell progression in HG-cultured podocytes

To determine the relationship between miR-27a-3p and *TIMP3* in regulating podocyte injury, podocytes were treated with in-miR-NC, in-miR-27a-3p, in-miR-27a-3p+si-NC or in-miR-27a-3p+si-*TIMP3* followed by exposure to HG for 36 h. As shown in Figure 6A, in-miR-27a-3p transfection elevated the protein level of *TIMP3* in HG-induced podocytes, but si-*TIMP3*

transfection restored the elevation. MiR-27a-3p inhibition distinctly suppressed cell apoptosis in HG-induced podocytes, while *TIMP3* deficiency reversed the effect (Figure 6B). Western blot assay showed that levels of α-smooth muscle actin (SMA), fibronectin (FN), and Type 1 collagen (Col I) was reduced and the level of podocin was increased by miR-27a-3p inhibition in HG-induced podocytes, whereas the impacts were reversed by decreasing *TIMP3* expression (Figure 6C). ELISA assay showed that the secreted levels of inflammatory cytokines were reduced in HG-induced podocytes following inhibition of miR-27a-3p, while *TIMP3* silencing abated the effects (Figure 6D–6F). To sum up, miR-27a-3p inhibition abated injury to HG-cultured podocytes by targeting *TIMP3*.
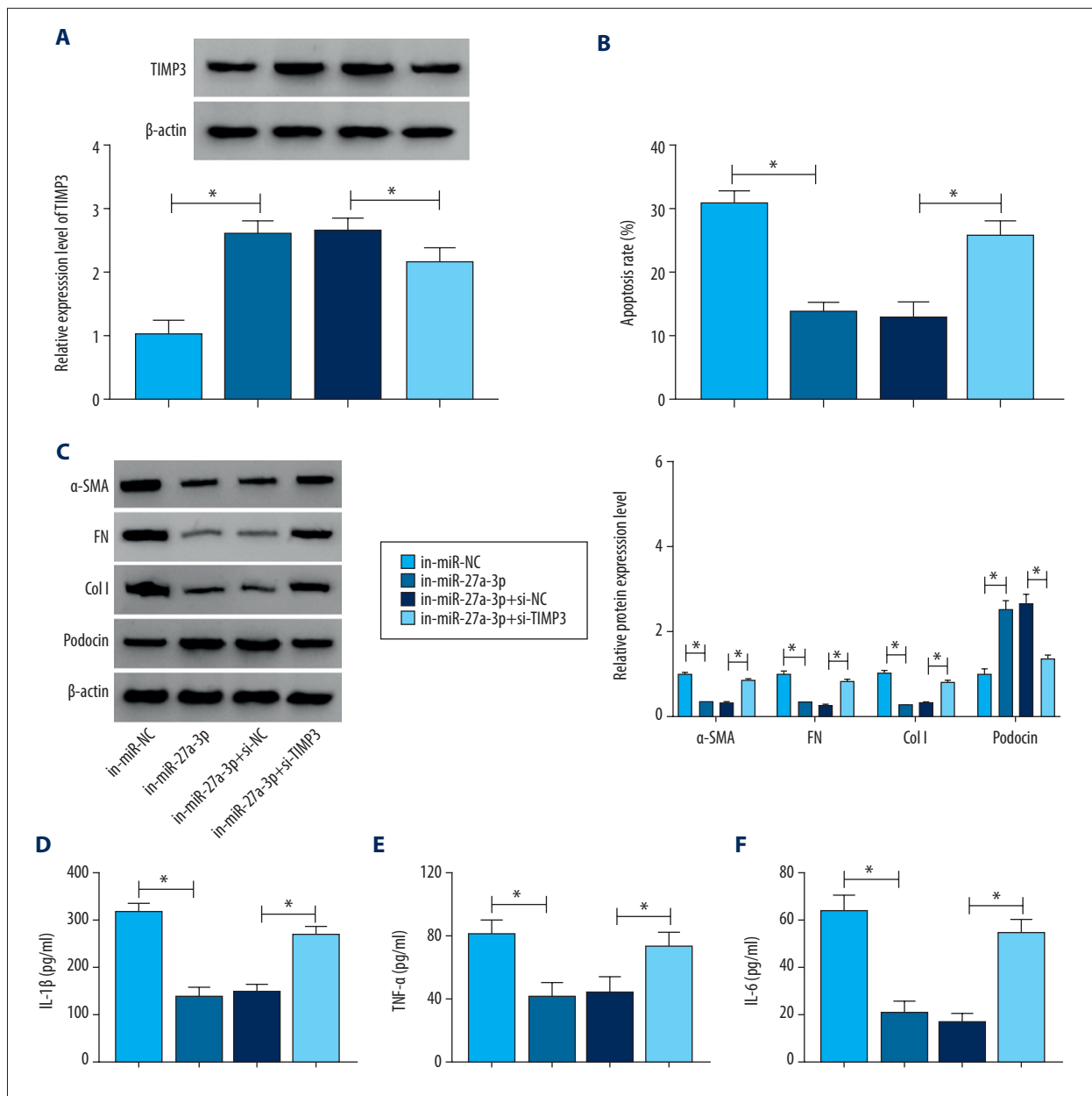
Figure 6. *TIMP3* knockdown reversed the suppressive roles of miR-27a-3p inhibition in cell apoptosis, fibrosis, and inflammation in HG-stimulated podocytes. Podocytes were introduced with in-miR-NC, in-miR-27a-3p, in-miR-27a-3p+si-NC or in-miR-27a-3p+si-*TIMP3* followed by HG treatment. (**A**) The protein level of *TIMP3* in HG-induced podocytes was measured by Western blot assay. (**B**) Cell apoptosis in HG-induced podocytes was assessed by flow cytometry analysis. (**C**) The protein levels of α-SMA, FN, Col I, and podocin in HG-induced podocytes were detected via Western blot assay. (**D–F**) Levels of IL-1β, TNF-α, and IL-6 were determined with ELISA kits. * P<0.05.

Discussion

Abnormal glucose metabolism, inflammation, fibrosis, and podocyte injury have been shown to be important factors in the pathogenesis of DN [17,18]. HG-induced podocytes have been used extensively to investigate DN progression [19,20]. We created DN cell models by exposing podocytes to 30-mM glucose for 36 h. LncRNAs have emerged as critical regulators in DN development. The goal of our research was to clarify the biological roles of 4930556M19Rik in HG-mediated podocytes. We verified that 4930556M19Rik overexpression could rescue HG-stimulated podocyte damage by regulating miR-27a-3p/*TIMP3* axis.

lncRNAs have been shown to exert their functions on DN through a mechanism involving competition with endogenous RNAs (ceRNAs) [21,22]. For example, Zha. reported that lncRNA maternally expressed gene3 (*MEG3*) increased with time and glucose concentration in HG-treated MCs and facilitated inflammation and fibrosis in DN by targeting miR-181a [23]. Liu et al. discovered that lncRNA metastasis-associated lung adenocarcinoma transcript 1 (MALAT1) contributed to HG-triggered injury in HK-2 cells by interacting with miR-145 [6]. Bai et al. claimed that LINC01619 was reduced in DN and its deficiency promoted oxidative stress and podocyte apoptosis via modulation of the miR-27a/Forkhead Box O1 (FOXO1) axis [12]. Herein, we observed that 4930556M19Rik level was reduced by HG exposure in a dose- or time-independent manner, which was consistent with the study by Li et al. [7]. Then gain-of-function studies were carried out to determine the precise roles of 4930556M19Rik in DN. We first verified that HG-trigged podocyte apoptosis was effectively restrained by elevation of 4930556M19Rik. Then we explored the impact of 4930556M19Rik on fibrosis of HG-cultured podocytes by measuring protein levels of the main markers of fibrosis via Western blot assay. As a result, HG-triggered α-SMA, FN, and Col I levels were all obviously rescued by overexpression of 4930556M19Rik in podocytes. Podocin is an important part of the glomerular filtration barrier, which plays vital roles in the normal structure and function of podocytes [24]. Here, we observed that HG treatment decreased the level of podocin, but the effect was abolished by elevating 4930556M19Rik. Moreover, ELISA assay demonstrated that HG-stimulated inflammatory cytokines were restored by 4930556M19Rik in podocytes. Taken together, 4930556M19Rik could reverse the injury to podocytes mediated by HG.

Subsequently, we further determined the underlying mechanism of 4930556M19Rik in modulation of HG-mediated podocyte injury. 4930556M19Rik was found to act as the sponge

for miR-27a-3p and miR-27a-3p was enhanced in HG-cultured podocytes. Moreover, miR-27a-3p inhibition repressed cell apoptosis, fibrosis, and inflammatory response in HG-treated podocytes. Podocyte damage mediated by 4930556M19Rik was ameliorated by elevating miR-27a-3p in HG-stimulated podocytes. In support of our findings, Zhou et al. reported that miR-27a level was increased by HG treatment in podocytes and aggravated injury to podocytes in HG [13]. Hou et al. suggested that miR-27a played a promoter role in fibrosis of renal tubulointerstitial in DN by inhibiting peroxisome proliferator-activated receptor-gamma (PPARγ) [25].

In addition, we demonstrated that 4930556M19Rik served as a ceRNA of miR-27a-3p to modulate *TIMP3* expression. *TIMP3* has been identified as the target of diverse miRNAs, such as miR-222 [26], miR-17-5p [27], and miR-323-3p [28]. Moreover, *TIMP3* has been documented to take part in regulating DN development [14,29]. Our results revealed for the first time that *TIMP3* was the target of miR-27a-3p and *TIMP3* silencing lessened the impact of miR-27a-3p inhibition on podocyte injury in HG. Our data illustrate that miR-27a-3p participates in DN development by targeting *TIMP3*.

Conclusions

In summary, HG led to a decrease in 4930556M19Rik level in podocytes. 4930556M19Rik overexpression reversed HG-triggered cell apoptosis, fibrosis, and inflammation by regulating the miR-27a-3p/*TIMP3* axis. Our study might provide a basis for research on the pathogenesis of DN. Moreover, our research provided novel insight into the molecular mechanism of 4930556M19Rik in DN and indicates that 4930556M19Rik may serve as a biomarker in DN. However, we did not verify our results *in vivo*, which should be considered in the future.

References:

1. Ha SK: ACE insertion/deletion polymorphism and diabetic nephropathy: Clinical implications of genetic information. J Diabetes Res, 2014; 2014: 846068

2. Najafian B, Alpers CE, Fogo AB: Pathology of human diabetic nephropathy. Contrib Nephrol, 2011; 170: 36–47

3. Alicic RZ, Johnson EJ, Tuttle KR: SGLT2 inhibition for the prevention and treatment of diabetic kidney disease: A review. Am J Kidney Dis, 2018; 72: 267–77

4. Mercer TR, Dinger ME, Mattick JS: Long non-coding RNAs: Insights into functions. Nat Rev Genet, 2009; 10: 155–59

5. Ma J, Zhao N, Du L et al: Downregulation of lncRNA NEAT1 inhibits mouse mesangial cell proliferation, fibrosis, and inflammation but promotes apoptosis in diabetic nephropathy. Int J Clin Exp Pathol, 2019; 12: 1174–83

6. Liu B, Qiang L, Wang GD et al: LncRNA MALAT1 facilities high glucose induced endothelial to mesenchymal transition and fibrosis via targeting miR-145/ZEB2 axis. Eur Rev Med Pharmacol Sci, 2019; 23: 3478–86

7. Li A, Peng R, Sun Y et al: LincRNA 1700020I14Rik alleviates cell proliferation and fibrosis in diabetic nephropathy via miR-34a-5p/Sirt1/HIF-1alpha signaling. Cell Death Dis, 2018; 9: 461

8. He L, Hannon GJ: MicroRNAs: Small RNAs with a big role in gene regulation. Nat Rev Genet, 2004; 5: 522–31

9. Gao BH, Wu H, Wang X et al: MiR-30c-5p inhibits high glucose-induced EMT and renal fibrogenesis by down-regulation of JAK1 in diabetic nephropathy. Eur Rev Med Pharmacol Sci, 2020; 24: 1338–49

10. Fu Y, Wang C, Zhang D et al: miR-15b-5p ameliorated high glucose-induced podocyte injury through repressing apoptosis, oxidative stress, and inflammatory responses by targeting Sema3A. J Cell Physiol, 2019; 234: 20869–78

11. Zha F, Bai L, Tang B et al: MicroRNA-503 contributes to podocyte injury via targeting E2F3 in diabetic nephropathy. J Cell Biochem, 2019; 120: 12574–81

12. Bai X, Geng J, Li X et al: Long noncoding RNA LINC01619 regulates microRNA-27a/Forkhead box protein O1 and endoplasmic reticulum stress-mediated podocyte injury in diabetic nephropathy. Antioxid Redox Signal, 2018; 29: 355–76

13. Zhou Z, Wan J, Hou X et al: MicroRNA-27a promotes podocyte injury via PPARgamma-mediated beta-catenin activation in diabetic nephropathy. Cell Death Dis, 2017; 8: e2658

14. Basu R, Lee J, Wang Z et al: Loss of *TIMP3* selectively exacerbates diabetic nephropathy. Am J Physiol Renal Physiol, 2012; 303: F1341–52

15. Kassiri Z, Oudit GY, Kandalam V et al: Loss of *TIMP3* enhances interstitial nephritis and fibrosis. J Am Soc Nephrol, 2009; 20: 1223–35

16. Fiorentino L, Cavalera M, Mavilio M et al: Regulation of *TIMP3* in diabetic nephropathy: A role for microRNAs. Acta Diabetol, 2013; 50: 965–9

17. Susztak K, Raff AC, Schiffer M et al: Glucose-induced reactive oxygen species cause apoptosis of podocytes and podocyte depletion at the onset of diabetic nephropathy. Diabetes, 2006; 55: 225–33

18. Wada J, Makino H: Inflammation and the pathogenesis of diabetic nephropathy. Clin Sci (Lond), 2013; 124: 139–52

19. Chen X, Zhao L, Xing Y et al: Down-regulation of microRNA-21 reduces inflammation and podocyte apoptosis in diabetic nephropathy by relieving the repression of *TIMP3* expression. Biomed Pharmacother, 2018; 108: 7–14

20. Long J, Wang Y, Wang W et al: MicroRNA-29c is a signature microRNA under high glucose conditions that targets Sprouty homolog 1, and its *in vivo* knockdown prevents progression of diabetic nephropathy. J Biol Chem, 2011; 286: 11837–48

21. Liz J, Esteller M: lncRNAs and microRNAs with a role in cancer development. Biochim Biophys Acta, 2016; 1859: 169–76

22. Yoon JH, Abdelmohsen K, Gorospe M: Functional interactions among microRNAs and long noncoding RNAs. Semin Cell Dev Biol, 2014; 34: 9–14

23. Zha F, Qu X, Tang B et al: Long non-coding RNA MEG3 promotes fibrosis and inflammatory response in diabetic nephropathy via miR-181a/Egr-1/TLR4 axis. Aging (Albany NY), 2019; 11: 3716–30

24. Greka A, Mundel P: Cell biology and pathology of podocytes. Annu Rev Physiol, 2012; 74: 299–323

25. Hou X, Tian J, Geng J et al: MicroRNA-27a promotes renal tubulointerstitial fibrosis via suppressing PPARgamma pathway in diabetic nephropathy. Oncotarget, 2016; 7: 47760–76

26. Zhang Y, Yang J, Zhou X et al: Knockdown of miR-222 inhibits inflammation and the apoptosis of LPS-stimulated human intervertebral disc nucleus pulposus cells. Int J Mol Med, 2019; 44: 1357–65

27. Peng H, Li H: The encouraging role of long noncoding RNA small nuclear RNA host gene 16 in epithelial-mesenchymal transition of bladder cancer via directly acting on miR-17-5p/metalloproteinases 3 axis. Mol Carcinog, 2019; 58: 1465–80

28. Zhang J, Lang Y, Guo L et al: MicroRNA-323a-3p Promotes Pressure Overload-Induced Cardiac Fibrosis by Targeting *TIMP3*. Cell Physiol Biochem, 2018; 50: 2176–87

29. Zhu FX, Wu HL, Chen JX et al: Dysregulation of microRNA-181b and *TIMP3* is functionally involved in the pathogenesis of diabetic nephropathy. J Cell Physiol, 2019; 234: 18963–69